Bimodal dynamics of mechanically constrained hydrogen bonds revealed by vibrational photon echoes

Bodis, P.; Yeremenko, S.; Berna, J.; Buma, W.J.; Leigh, D.A.; Woutersen, S.

DOI
10.1063/1.3569761

Publication date
2011

Document Version
Final published version

Published in
Journal of Chemical Physics

Bimodal dynamics of mechanically constrained hydrogen bonds revealed by vibrational photon echoes

Pavol Bodis,[1] Sergiy Yeremenko,[1] José Berná,[2,a)] Wybren J. Buma,[1,b)] David A. Leigh,[2,b)] and Sander Woutersen[1,b)]
[1]*Van 't Hoff Institute for Molecular Sciences, University of Amsterdam, Science Park 904, 1098 XH Amsterdam, The Netherlands*
[2]*School of Chemistry, University of Edinburgh, The King's Buildings, West Mains Road, Edinburgh EH9 3JJ, United Kingdom*

(Received 14 December 2010; accepted 3 March 2011; published online 4 April 2011)

We have investigated the dynamics of the hydrogen bonds that connect the components of a [2]rotaxane in solution. In this rotaxane, the amide groups in the benzylic-amide macrocycle and the succinamide thread are connected by four equivalent N−H···O=C hydrogen bonds. The fluctuations of these hydrogen bonds are mirrored by the frequency fluctuations of the NH-stretch modes, which are probed by means of three-pulse photon-echo peak shift spectroscopy. The hydrogen-bond fluctuations occur on three different time scales, with time constants of 0.1, 0.6, and ≥200 ps. Comparing these three time scales to the ones found in liquid formamide, which contains the same hydrogen-bonded amide motif but without mechanical constraints, we find that the faster two components, which are associated with small-amplitude fluctuations in the strength of the N−H···O=C hydrogen bonds, are very similar in the liquid and the rotaxane. However, the third component, which is associated with the breaking and subsequent reformation of hydrogen bonds, is found to be much slower in the rotaxane than in the liquid. It can be concluded that the mechanical bonding in a rotaxane does not influence the amplitude and time scale of the small-amplitude fluctuations of the hydrogen bonds, but strongly slows down the complete dissociation of these hydrogen bonds. This is probably because in a rotaxane breaking of the macrocycle–axle contacts is severely hindered by the mechanical constraints. The hydrogen-bond dynamics in rotaxane-based molecular machines can therefore be regarded as liquidlike on a time scale 1 ps and less, but structurally frozen on longer (up to at least 200 ps) time scales. © *2011 American Institute of Physics*. [doi:10.1063/1.3569761]

I. INTRODUCTION

Rotaxanes and catenanes (molecules in which the components are mechanically linked but not connected by covalent bonds) are proving useful structural prototypes for helping realize the concept of artificial molecular machinery.[1–10] Whilst it is tempting to regard such multicomponent assemblies as "molecular meccano,"[11] many aspects of classical mechanics become meaningless at this level of miniaturization.[12] For example, in the macroscopic world the equations of motion are governed by inertial terms (dependent on mass), but under the conditions that molecular machines operate viscous forces (governed by particle dimensions) and Brownian motion dominate mechanical behavior.[13,14] Such random (thermal) motions of the components are often an essential part of the functioning of many molecular devices, as is illustrated by rotaxane-based molecular machines in which translation of the macrocycle from one binding site on the thread to another requires rare equilibrium fluctuations to simultaneously break several hydrogen bonds that bind the macrocycle to its initial binding site.[4,15–19] Although the dynamics of catenane- and rotaxane-based systems have been extensively studied on the second and millisecond time scales,[16,20] the fundamental motions within their components, and the thermal fluctuations in the surrounding medium take place in the picosecond or subpicosecond time domain. In order to understand how such elementary motions of individual functional groups determine the global behavior of relatively massive (>500 D) mechanically linked fragments, it is necessary to have a "quantum tool" that provides detailed insight into both structure and dynamics on such time scales. Infrared ultrafast spectroscopy is ideally suited for this purpose since it allows localized molecular vibrations to be probed with femtosecond temporal resolution.[21,22] Here we employ this technique to investigate the ultrafast intercomponent fluctuations in a [2]rotaxane consisting of a succinamide-based thread and a benzylic-amide-based macrocycle.[4,15,17,23] The experiments reveal that mechanical bonding in a rotaxane has little effect on the amplitude or rate of (sub)picosecond fluctuations of the intercomponent hydrogen bonds, but that it decreases the rate of spontaneous breaking and remaking of these hydrogen bonds by more than an order of magnitude.

The [2]rotaxane we investigate has a geometry reminiscent of a cartwheel (see Fig. 1), with the macrocycle

a)Current address: Departamento de Química Orgánica, Facultad de Química, Universidad de Murcia, Campus Espinardo, E-30100 Murcia, Spain.
b)Authors to whom correspondence should be addressed. Electronic addresses: david.leigh@ed.ac.uk, w.j.buma@uva.nl, and s.woutersen@uva.nl.

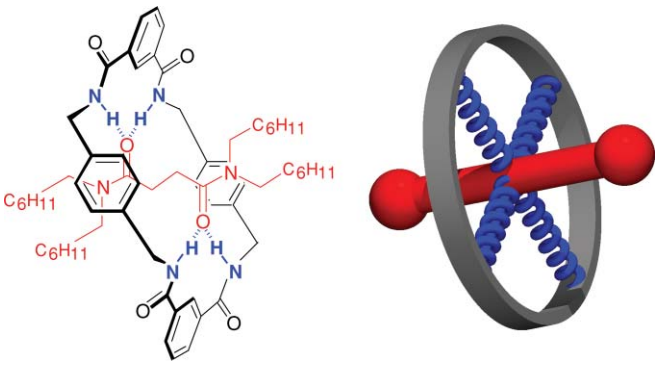

FIG. 1. Chemical structure of the investigated [2]rotaxane, and a schematic representation with color coding of the rim (gray), spokes (blue), and axle (red).

representing the rim, and the thread the axle. Four hydrogen bonds act as spokes which maintain the position of the rim with respect to the axle. To probe the conformational fluctuations of the rotaxane, we selected the NH-stretch vibrational mode, which has a frequency of 3370 cm^{-1} (see the absorption spectrum in Fig. 2). This mode involves stretching of the N−H bonds participating in the N−H···O=C hydrogen bonds that connect the rim and the axle of the "cartwheel." The instantaneous length of an N−H···O=C hydrogen bond determines the instantaneous frequency of the NH-stretch mode, and there exists an approximately linear relation between these quantities.[24–26] Hence, the fluctuations of the NH-stretch frequency directly reflect fluctuations in the intercomponent distances in the rotaxane. These frequency fluctuations can be probed using the vibrational photon-echo peak shift technique (PEPS).[27–29] It can be shown[30] that the photon-echo peak shift mirrors the frequency correlation function $M(t) = \langle \delta\omega_{NH}(t)\delta\omega_{NH}(0)\rangle$, where $\delta\omega_{NH}(t) = \omega_{NH}(t) - \langle\omega_{NH}\rangle$ is the time dependent deviation of NH-stretch frequency from its average value $\langle\omega_{NH}\rangle$. This correlation function characterizes the time scales and amplitudes of the NH-stretch frequency fluctuations, and hence of the

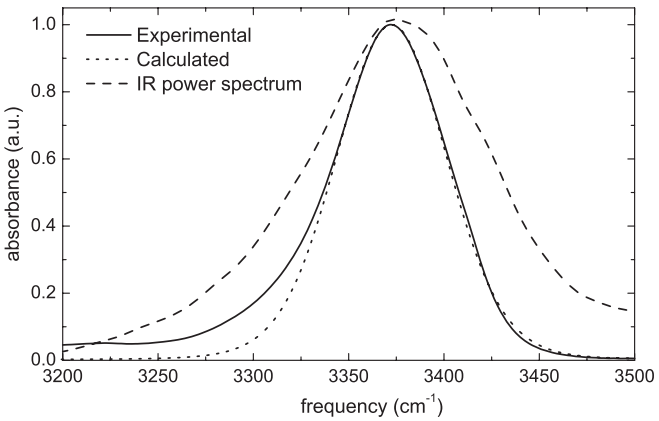

FIG. 2. FTIR absorption spectrum of a 10 mM solution of the rotaxane in $CDCl_3$ (solid line). The dotted line is a simulated spectrum (using the parameters of Table I). The dashed line represents the spectrum of the IR pulses used for the PEPS and pump–probe experiments.

fluctuations in the length of the intercomponent NH···OC hydrogen bonds.

The rotaxane we investigate contains four NH groups in relatively close proximity. For this reason it is essential to know whether, and to what extent the NH-stretch excitation is delocalized over the NH groups. This investigation forms the first half of the article. It turns out that the NH-stretch excitation remains essentially localized on a single NH-bond during the first few picoseconds after excitation. Hence, the fast NH-stretch frequency fluctuations which are probed using the photon-echo peak shift method in the second half of the article, directly reflect the fluctuations of individual hydrogen bonds in the [2]rotaxane.

II. MATERIALS AND METHODS

For the pump–probe and PEPS experiments we use an infrared generation setup described previously.[31] Briefly, infrared laser pulses with a duration of ~90 fs, an energy of ~10 μJ and a spectrum centered at 3400 cm^{-1} (FWHM ~120 cm^{-1}) are generated with a home-built BBO/KTP based white-light seeded optical parametric amplifier (OPA). The OPA is pumped by a Ti:Sapphire laser/amplifier system (Spectra Physics Hurricane). In the PEPS experiment the mid-IR output of the OPA is split into four parts to obtain three excitation beams of approximately equal intensity with wave vectors $\vec{k}_1$, $\vec{k}_2$, and $\vec{k}_3$, and a fourth beam (5% of the total power) which is used to continuously monitor the excitation spectrum using a spectrograph and HgCdTe array detector. The three excitation beams are focused into the sample using a boxcars geometry and recollimated after it by means of two off-axis parabolic mirrors. The photon-echo signals are generated in conjugated phase-matched directions $\vec{k}_s = \vec{k}_3 + \vec{k}_2 - \vec{k}_1$ and $\vec{k}'_s = \vec{k}_3 + \vec{k}_1 - \vec{k}_2$, and are detected simultaneously with two HgCdTe detectors, while scanning both the coherence time τ between $\vec{k}_1$ and $\vec{k}_2$ and the waiting time T between $\vec{k}_2$ and $\vec{k}_3$. To suppress background scattering, we chop the $\vec{k}_1$ beam at half the laser repetition rate and use lock-in amplification to detect the photon-echo signals. Photon-echo peak shift measurements are performed by measuring at which value of τ the time-integrated echo-signal reaches its maximum for a series of waiting times T.[32] Transient-grating experiments are carried out by setting $\tau = 0$ and recording the time-integrated intensity in the phase-matched directions as a function of T.[33]

In the pump–probe experiments, we resonantly excite the NH-stretch mode, and monitor the subsequent vibrational relaxation process by measuring the frequency-dependent absorption change as a function of delay time. We use the same setup for the mid-infrared generation. Small fractions (5%) of the light reflected from the front and back surfaces of a wedged CaF_2 window are used as probe and reference pulses, the remainder is used as the pump pulse. The pump and probe pulses are focused and overlapped in the sample by means of a 100 mm off-axis parabolic mirror. Transient absorption changes are measured by frequency-dispersed detection of probe and reference pulses using a 32-element HgCdTe array detector. The transient-grating and PEPS experiments are carried out with parallel polarizations of the

pump and probe pulses; the pump–probe experiments are carried out with both parallel and perpendicular polarizations of the pump and probe pulses. From the absorption changes for parallel ($\Delta\alpha_{||}$) and perpendicular ($\Delta\alpha_{\perp}$) polarizations, we obtain the rotation-free signal as $\Delta\alpha_{\mathrm{RF}} = \Delta\alpha_{||} + 2\Delta\alpha_{\perp}$, and the anisotropy as $R = (\Delta\alpha_{||} - \Delta\alpha_{\perp})/\Delta\alpha_{\mathrm{RF}}$.

The synthesis and characterization of the thread and the benzylic amide [2]rotaxane are described in the supplementary material.[34] The axle of the investigated [2]rotaxane contains four cyclohexyl residues (C_6H_{11}) which prevent the dethreading of the macrocycle. In addition, the incorporation of these aliphatic stoppers improves the solubility of the interlocked molecule in halogenated solvents in comparison to previously investigated rotaxanes with aromatic stoppers.[23,31] All experiments are performed at room temperature on 10 mM solution of the [2]rotaxane in $CDCl_3$ kept between two CaF_2 windows using a 1 mm thick spacer.

III. RESULTS AND DISCUSSION

A. Localized character of the NH-stretch excitations

The steady-state absorption spectrum of a 10 mM solution of the [2]rotaxane in $CDCl_3$ and the power spectrum of the pulses used for the pump–probe and photon-echo experiments are shown in Fig. 2.

The rotaxane contains four NH groups, but there is only a single peak in the steady-state absorption spectrum (at 3370 cm^{-1}). This suggests that the coupling between the NH-stretch modes is smaller than the inhomogeneous broadening. If the coupling were larger, there would be a significant splitting between the symmetric and antisymmetric NH-stretch modes resulting in a double peak in the steady-state absorption spectrum.

To estimate the value of the coupling between the two neighboring NH-stretch modes, we can use the dipole–dipole approximation for the coupling strength β between vibrational modes a and b,

$$\beta = \frac{1}{4\pi\varepsilon_0}\left[\frac{\vec{\mu}_a\cdot\vec{\mu}_b}{|\vec{r}|^3} - 3\frac{(\vec{r}\cdot\vec{\mu}_a)(\vec{r}\cdot\vec{\mu}_b)}{|\vec{r}|^5}\right], \quad (1)$$

where $\vec{\mu}_{a,b}$ are the transition-dipole moments of the neighboring NH-stretch modes, and $\vec{r}$ is the distance vector between the two transition dipoles. We find that for the closest NH groups (~4 Å) the coupling strength β is 1.15 cm^{-1}. We have also determined the coupling using a density-functional theory calculation at the B3LYP/6-31G* level, and find it to be 0.85 cm^{-1}, in good agreement with the value obtained using the dipole–dipole approximation. This coupling is much smaller than the width of the absorption band (~150 cm^{-1}), so the NH-stretch excitation is essentially localized on a single NH group.

B. Population relaxation and resonant vibrational energy transfer

Figure 3 shows the absorption change upon resonant excitation of the NH-stretch mode as a function of the probe frequency for several delays between the pump and probe pulse. The negative absorption change at the $v = 0 \rightarrow 1$ frequency is due to $v = 0 \rightarrow 1$ bleaching and $v = 1 \rightarrow 0$ stimulated emission, and the positive absorption change at lower frequency is due to $v = 1 \rightarrow 2$ excited-state absorption. The signal decays with increasing delay time due to population relaxation (see Fig. 4), and shows a small offset for long delays. This residual signal is due to heating (less than 1 K, as determined from the focal size, pulse energy, and specific heat of the solvent) of the sample upon vibrational relaxation of the NH-stretch mode. For the delays investigated in the photon-echo experiments (≤3 ps), the residual signal is sufficiently small compared to the nonlinear signal caused by the $v = 1$ population that it can be neglected in the analysis of the data.[35] To avoid contributions from the instantaneous solvent response (cross-phase modulation), only data points for delays longer than 0.3 ps are used in the data analysis. The power spectrum of the infrared pulses used to excite and probe the sample is broader than the absorption spectrum.

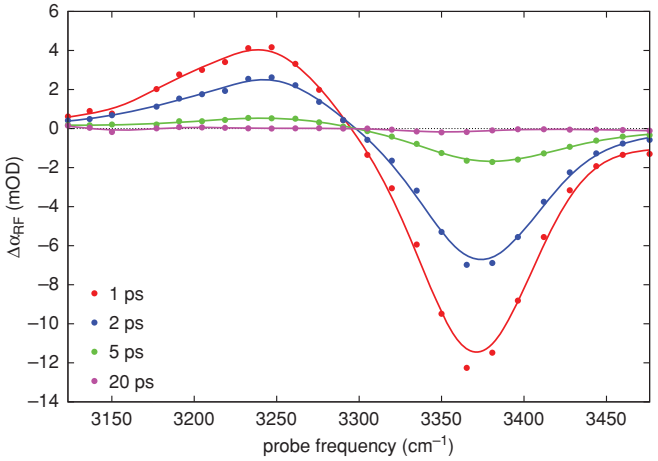

FIG. 3. Rotation-free absorption change $\Delta\alpha_{\mathrm{RF}} = \Delta\alpha_{||} + 2\Delta\alpha_{\perp}$ upon resonant excitation of the NH-stretch mode vs probe frequency for several values of the delay between the pump and probe pulses. The curves are a guide to the eye.

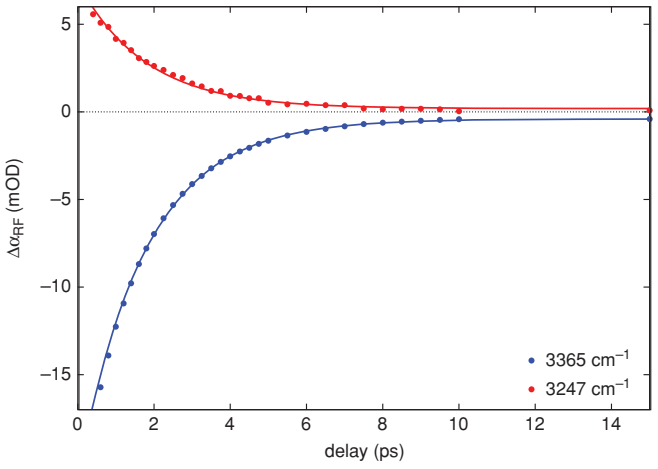

FIG. 4. Decay of the rotation-free pump–probe signal $\Delta\alpha_{\mathrm{RF}} = \Delta\alpha_{||} + 2\Delta\alpha_{\perp}$ as a function of delay between the pump and probe pulse for both bleaching (at 3380 cm^{-1}) and induced absorption (at 3218 cm^{-1}). The curves are a least-squares fit to an exponential decay with $T_1 = 1.77 \pm 0.02$ ps.

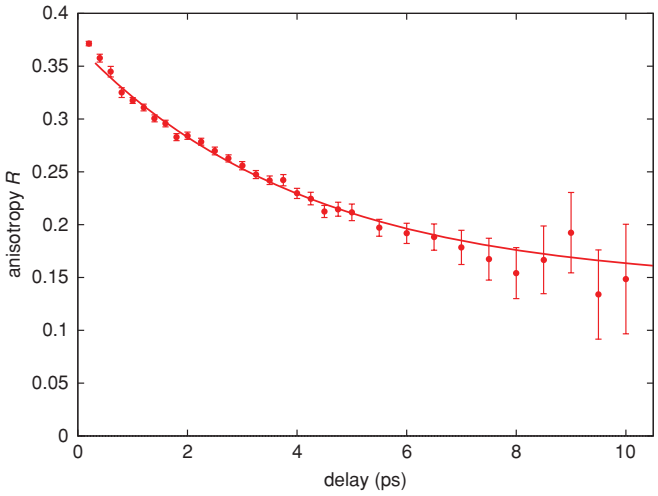

FIG. 5. NH-stretch anisotropy decay at a probe frequency of 3365 cm^{-1}. The curve is the result of a least-squares fit to an exponential decay, with $\tau = 4.1 \pm 0.6$ ps.

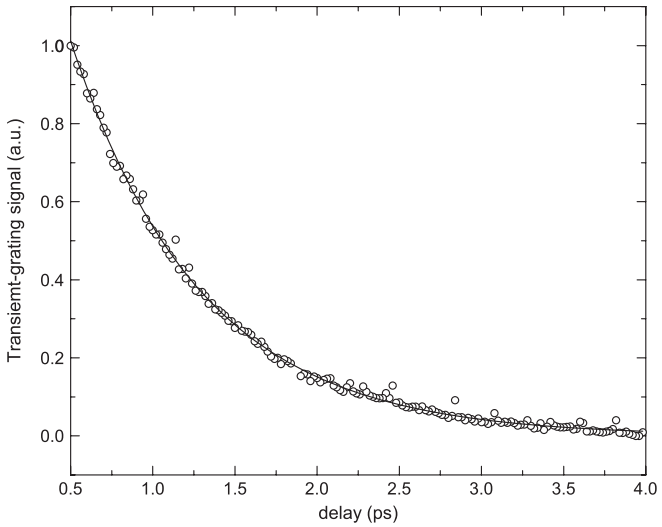

FIG. 6. Decay of the transient-grating signal as a function of delay between the two pulses that create the population grating and the third pulse that is diffracted from it. Data recorded with parallel polarizations of the three IR pulses.

Hence, no hole burning occurs and spectral diffusion does not influence the pump–probe data, so that the decay of the rotation-free pump–probe signal is determined by population relaxation only. From a least-squares fit of an exponential decay to the decay of the rotation-free pump–probe signal (see curves in Fig. 4) we obtain an NH-stretch excited-state population lifetime T_1 of 1.77 ± 0.02 ps.

Figure 5 shows the decay of the NH-stretch anisotropy at a probe frequency of 3365 cm^{-1} for delays >0.2 ps (the data at shorter delays are influenced by contributions from the solvent response). The decay of the anisotropy can be well described by a single-exponential decay with a time constant of 4.1 ± 0.6 ps. The anisotropy decay can be caused by rotation of the whole molecule, and/or by energy transfer of the NH-stretch excitation between the NH groups. To estimate the time scale expected for the former process, we use the Stokes–Einstein model.[36] In this model, the anisotropy decays as a single exponential for orientational diffusion of a spherical molecule with a time constant τ that is a direct measure of its diffusion coefficient D,

$$\tau = \frac{4\pi R^3 \eta}{3k_B T}, \tag{2}$$

where R is the Stokes radius of the spherical molecule, η is the viscosity, k_B is the Boltzmann constant, and T is the temperature. From x-ray studies,[23] we find the size of the [2]rotaxane to be ~2 nm. Assuming a spherical shape with the Stokes radius of 1 nm, we estimate the orientational relaxation time to be ~400 ps. Therefore, rotational diffusion of the entire molecule cannot explain the observed anisotropy decay.

The second explanation could be resonant (Förster) energy transfer of the NH-stretch excitation between NH groups. The rate of this energy transfer is given by[37,38]

$$k_{\text{Förster}} = \frac{|\vec{\mu}_a|^2 |\vec{\mu}_b|^2 \kappa^2}{16\pi^2 n^4 \epsilon_0^2 \hbar^2 c R^6} \int \sigma_a(\tilde{\nu}) \sigma_b(\tilde{\nu}) d\tilde{\nu}, \tag{3}$$

where n is the refractive index, R is the distance between dipoles, and $\sigma_{a,b}(\tilde{\nu})$ are the normalized absorption lineshapes with the frequency $\tilde{\nu} = 1/\lambda$ expressed in m^{-1}. The magnitude of the transition dipole moment $\vec{\mu}_{NH} = \vec{\mu}_a = \vec{\mu}_b$ can be obtained from the frequency-integrated absorption spectrum using[39]

$$|\vec{\mu}_{NH}|^2 = \frac{1}{4} \frac{3hc\epsilon_0 \ln 10 \int \epsilon(\tilde{\nu}) d\tilde{\nu}}{2\pi^2 \tilde{\nu}_0 N_A}, \tag{4}$$

where $\epsilon(\tilde{\nu})$ is the absorption coefficient of the NH-stretch mode (with the frequency $\tilde{\nu} = 1/\lambda$ expressed in m^{-1}) and $\tilde{\nu}_0$ is the frequency at the absorption maximum. The factor 1/4 in this equation accounts for the fact that there are 4 NH groups per molecule. By numerically integrating the experimental absorption spectrum we obtain $|\vec{\mu}_{NH}| = 0.135$ D, and from Eq. (3) we obtain a Förster transfer rate of 2.74 ns^{-1}, which corresponds to an anisotropy decay time of ~350 ps. This decay time is much slower than the experimentally observed decay of the anisotropy (Fig. 5), which suggests that the transfer involves not only dipolar but also through-bond interaction[40] or higher-order electrostatic interactions. The latter have been shown to play a significant role in the resonant vibrational energy transfer between HF and water in the liquid phase.[41]

The residual anisotropy observed at long delay times confirms that the anisotropy decay is caused by vibrational energy redistribution between the NH groups. It can be shown[42] that after energy redistribution from an initially excited mode a to two neighboring modes a and b, the value of anisotropy changes from a value of $\frac{2}{5}$ to $\frac{1}{5}(3\cos^2\theta_{ab} - 1)$, where θ_{ab} is the angle between the two neighboring transition dipoles. Using the crystallography value $\theta_{ab} \approx 77^\circ$ between the NH groups in the macrocycle, one expects the anisotropy to decay to a value of 0.13, in good agreement with the experimentally observed plateau value of 0.15.

The T_1 obtained from the pump–probe measurements is confirmed by a transient-grating experiment.[33] Figure 6 shows the intensity of the transient-grating signal as a function of delay T between the $\vec{k}_1, \vec{k}_2$ pulse pair that generates a

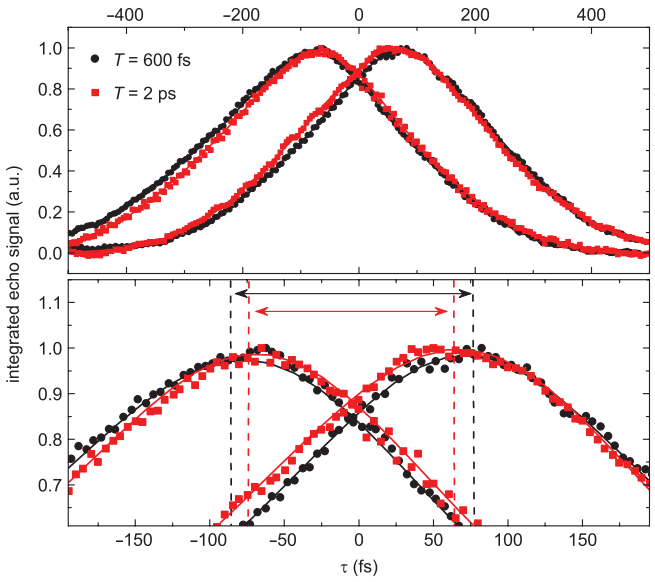

FIG. 7. Upper panel: photon-echo signals in the phase-matched directions $\vec{k}_3 + \vec{k}_2 - \vec{k}_1$ and $\vec{k}_3 - \vec{k}_2 + \vec{k}_1$ as a function of the coherence time τ, for waiting times T of 600 fs (black circles) and 2000 fs (red squares). Lower panel: close up showing the decrease of the photon-echo peak shift with increasing waiting time. The length of the horizontal arrows is twice the echo-peak shift.

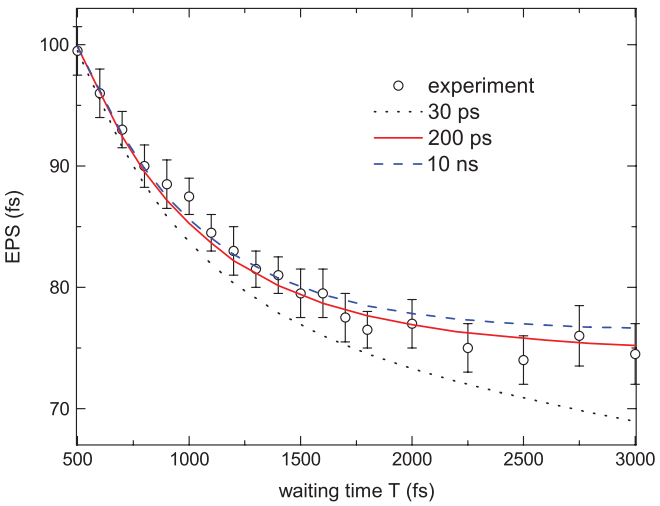

FIG. 8. Photon echo-peak shift data of the [2]rotaxane (○) and the modeled echo-peak shift (curves) for 30 ps, 200 ps, and 10 ns third time component.

population grating, and the $\vec{k}_3$ pulse which is diffracted from this grating.

Like the pump–probe signal, the transient-grating signal decays due to population relaxation. It can be fitted with a single-exponential decay with a time constant of 0.79 ± 0.01 ps. This time constant is half of the population lifetime T_1, because the transient-grating signal depends on the intensity of the third pulse, whereas the pump–probe signal on the amplitude of the probe field.[43] The observed population lifetime of 1.6 ps obtained from the transient-grating experiment is in good agreement with the value obtained using pump–probe spectroscopy.

C. Hydrogen-bond fluctuations

In order to investigate the frequency fluctuations of the NH-stretch mode we employ the three-pulse photon-echo peak-shift technique, which gives direct access to the frequency-correlation function of an optical transition.[27–29,35] In particular, the delay τ at which the integrated photon-echo signal is maximal (the echo-peak shift) plotted versus the waiting time T mirrors the correlation function of the frequency fluctuations.[32] Since the NH-stretch excitation is localized on a single NH group, the NH-stretch frequency fluctuations directly reflect the hydrogen-bond dynamics and thus the structural fluctuations of the macrocycle with respect to the thread.

The PEPS measurements were performed for waiting times T ranging from 500 fs to 3 ps, the accessible range being limited at short waiting times by the solvent response and at long waiting times by the population relaxation. The relatively long T_1 (1.6 ps) and marginal thermal residual observed in the pump–probe measurements allow us to observe the PEPS at comparatively long waiting times. The experimentally determined echo-peak shifts at the waiting times T of 600 and 2000 fs are shown in Fig. 7.

We use a least-squares fit of a Gaussian to the top of the echo signal to determine the position of the echo-peak maximum. The lower part of Fig. 7 shows a close-up of the maxima to illustrate the observed differences in the echo-peak maxima as a function of waiting time T. The two sets of data for both 600 and 2000 fs waiting times represent the echo signal detected in both phase-matched directions. In both echo peaks the signal is asymmetric with respect to $\tau = 0$, which indicates that the NH-stretch mode retains a certain part of the memory of its initial frequency for at least 2000 fs.

The observed PEPS as a function of waiting time is shown in Fig. 8. In the numerical analysis of the data, we use the Brownian oscillator model to describe the frequency-correlation function. Since the connection between the NH groups in the macrocycle is flexible, and the coupling between their stretching modes is small (see Sec. III A), we assume that their NH-stretch frequency fluctuations are uncorrelated.[44] Since the spectrum of the IR pulses (see Fig. 2) used in these experiments covers both transitions from the ground state and from the first excited state ($0 \rightarrow 1$ and $1 \rightarrow 2$), the numerical calculations have to be performed in the framework of a three-level system for the NH-stretch mode. The system–field interaction is then described by eight double-sided Feynman diagrams, three of which are responsible for rephasing, three for nonrephasing, and two for two-photon processes.[27,45,46] In our analysis, we quantitatively reproduce both the steady-state absorption spectrum and the PEPS signal using the same frequency-correlation function. We find that the data can be well described using a frequency-correlation function involving three overdamped Brownian oscillators,

$$M(t) = \langle \delta\omega_{NH}(t)\delta\omega_{NH}(0)\rangle = \Delta_1^2 \exp(-\Lambda_1 t) + \Delta_2^2 \exp(-\Lambda_2 t) + \Delta_3^2 \exp(-\Lambda_3 t), \quad (5)$$

TABLE I. Time constants and amplitudes of the three components in the NH-stretch frequency correlation function in the rotaxane and in a dilute liquid CDONDH/$CDOND_2$ mixture (Ref. 47).

	[2]Rotaxane		Formamide[a]	
	$1/\Lambda_i$ (ps)	Δ_i^2(%)	$1/\Lambda_i$ (ps)	Δ_i^2(%)
Homogeneous component	0.1	32	0.24	54
Fast fluctuations	0.6	31	0.8	13
Slow fluctuations	$\geq$200	37	11	34

[a]Values taken from Ref. 47.

where $1/\Lambda_i$ and Δ_i (with $i = 1, 2, 3$) are the time constants and amplitudes of the three components of the frequency-correlation function. The simulation of the experimental data (both the absorption spectrum and the PEPS signal) was performed as an iterative process, in which the parameters of the response function were varied until the best fit of the calculation to the complete set of experimental data was achieved.

Figure 8 shows the comparison of the measured and the simulated integrated PEPS as a function of waiting time T. The simulated absorption spectrum is compared to the experimental one in Fig. 2. An overview of the fitted parameters describing the modeled frequency correlation function are listed in Table I. Since the experimental data of the PEPS start at 500 fs, it is evident that for a quantitative description we need only the second $1/\Lambda_2$ and the third $1/\Lambda_3$ component. However, in order to simulate both the steady-state absorption spectrum and the PEPS at the same time, we need to include the first component $1/\Lambda_1$ as well. We find that this component of the frequency-correlation function is essential for a proper simulation of the steady-state absorption spectrum. The third component involves a very slow decay, and to determine its dynamics we have tried several decay constants. As shown in Fig. 8, even a decay constant of 30 ps is not long enough to describe the experimental data quantitatively, so we can conclude that the dynamics involve a time scale significantly slower than 30 ps. We obtain a good quantitative description of the PEPS data using time constants greater than or equal to 200 ps for the slowest decay of the correlation function (see Fig. 8). A time constant of 10 ns for the slowest component (which is in practice equivalent to a constant offset in the correlation function, and leads to the same values for the time constants of the two faster components) also results in good agreement with the experimental data. Although it is thus possible to determine a lower limit for the time constant of the slowest component of the correlation function, it is not possible to determine an upper limit, because the T_1 population relaxation decay causes the echo-peak intensity to become too small to measure the PEPS accurately for waiting times $T > 3$ ps.

A multicomponent decay of the frequency correlation function has been observed previously for compounds containing similar hydrogen-bonded moieties. In particular, Park *et al.*[47] carried out 2D-IR and photon-echo measurements on the NH-stretch mode of a dilute mixture of CDONDH (formamide) in $CDOND_2$. Liquid formamide forms the same N−H···O=C hydrogen bonds as occur in the rotaxane, except for the mechanical bonding in the latter. Three components are observed in the NH-stretch frequency correlation function of liquid formamide, with time constants of 0.24, 0.8, and 11 ps (see Table I). Based on the observed decay of the NH-stretch anisotropy, Park *et al.* could assign the 11 ps time scale to the breaking (dissociation) and subsequent reformation of N−H···O=C hydrogen bonds, whereas the 0.8 and 0.24 ps components correspond to small-amplitude random variations in the hydrogen-bond length and angle. In the latter, small-amplitude H-bond fluctuations no dissociation of the hydrogen bond occurs. Comparing the NH-stretch correlation function of liquid formamide to that of the [2]rotaxane, we find that the time scales and relative amplitudes of the two fast components of the hydrogen-bond fluctuations are very similar in the two systems. However, the third component is much slower in the rotaxane. This implies that the fast (<1 ps) fluctuations of the N−H···O=C hydrogen bonds are independent of whether or not the two hydrogen-bonded moieties are mechanically interlocked, but that complete breaking (and subsequent reformation) of hydrogen bond occurs on a much slower time scale in the rotaxane than in the unconstrained hydrogen-bonded system. This can be explained as follows: in the rotaxane, the macrocycle is locked onto the thread by four hydrogen bonds in such a way that breaking only one of the hydrogen bonds will result in considerable straining of the structure. The only way to break hydrogen bonds whilst retaining the energetically most favorable conformation of the macrocycle is to break all four hydrogen bonds simultaneously. As this process will occur very rarely, the third, ~10 ps component observed in the hydrogen-bond dynamics of liquid formamide will be much slower in the rotaxane.

IV. CONCLUSION

To conclude, we have used time-resolved vibrational spectroscopy to study picosecond hydrogen-bond fluctuations in a molecular wheel–axle system. Our results show that the mechanical constraint of the macrocycle/thread system has no significant influence on the subpicosecond fluctuations of the hydrogen bonds. However, the rate of spontaneous breaking and remaking of hydrogen bonds is slowed down by more than an order of magnitude by the mechanical rigidity of the rotaxane. Thus, on a time scale of less than a picosecond the hydrogen bonds that connect the rim and axle of a rotaxane-based "molecular wheel" behave in the same way as N−H···O=C hydrogen bonds in a liquid. However, the hydrogen-bond breaking and remaking dynamics, which occurs on a 10 ps time scale in the liquid phase, turns out to be much slower for the hydrogen bonds in a mechanically bonded system.

ACKNOWLEDGEMENTS

The authors kindly thank Matthijs Panman for critically reading the manuscript. This work was supported by the European Community (EMMMA IHP Research Training Network, Contract No. HPRN-CT-2002-00168, and Hy3M STREP, Contract No. NMP4-CT-2004-013525) and by the

Stichting voor Fundamenteel Onderzoek der Materie (FOM), which is financially supported by the Nederlandse Organisatie voor Wetenschappelijk Onderzoek (NWO).

[1]C. P. Collier, G. Mattersteig, E. W. Wong, Y. Luo, K. Beverly, J. Sampaio, F. M. Raymo, J. F. Stoddart, and J. R. Heath, Science **289**, 1172 (2000).
[2]V. Balzani, A. Credi, F. M. Raymo, and J. F. Stoddart, Angew. Chem., Int. Ed. **39**, 3349 (2000).
[3]B. L. Feringa, Nature (London) **408**, 151 (2000).
[4]D. A. Leigh, J. K.Y. Wong, F. Dehez, and F. Zerbetto, Nature (London) **424**, 174 (2003).
[5]P. Thordarson, E. J. A. Bijsterveld, A. E. Rowan, and R. J. M. Nolte, Nature (London) **424**, 915 (2003).
[6]J. D. Badjić, V. Balzani, A. Credi, S. Silvi, and J. F. Stoddart, Science **303**, 1845 (2004).
[7]R. A. van Delden, M. K.J. van der Wiel, M. M. Pollard, J. Vicario, N. Koumoura, and B. L. Feringa, Nature (London) **437**, 1337 (2005).
[8]S. P. Fletcher, F. Dumur, M. M. Pollard, and B. L. Feringa, Science **310**, 80 (2005).
[9]J. E. Green, J. W. Choi, A. Boukai, Y. Bunimovich, E. Johnston-Halperin, E. DeIonno, Y. Luo, B. A. Sheriff, K. Xu, Y. S. Shin, H. R. Tseng, J. F. Stoddart, and J. R. Heath, Nature (London) **445**, 414 (2007).
[10]V. Serreli, C.-F. Lee, E. R. Kay, and D. A. Leigh, Nature (London) **445**, 523 (2007).
[11]J. F. Stoddart, Pure Appl. Chem. **77**, 1098 (2005).
[12]E. R. Kay, D. A. Leigh, and F. Zerbetto, Angew. Chem., Int. Ed. **46**, 72 (2007).
[13]E. Purcell, Am. J. Phys. **45**, 3 (1977).
[14]R. D. Astumian, Phys. Chem. Chem. Phys. **9**, 5067 (2007).
[15]A. M. Brouwer, C. Frochot, F. G. Gatti, D. A. Leigh, L. Mottier, F. Paolucci, S. Roffia, and G. W. H. Wurpel, Science **291**, 2124 (2001).
[16]F. G. Gatti, S. León, J. K. Y. Wong, G. Bottari, A. Altieri, M. A. F. Morales, S. J. Teat, C. Frochot, D. A. Leigh, A. M. Brouwer, *et al.*, Proc. Natl. Acad. Sci. U.S.A. **100**, 10 (2003).
[17]J. V. Hernandez, E. R. Kay, and D. A. Leigh, Science **306**, 1532 (2004).
[18]R. D. Astumian, Proc. Natl. Acad. Sci. U.S.A. **104**, 19715 (2007).
[19]M. R. Panman, P. Bodis, D. J. Shaw, B. H. Bakker, A. C. Newton, E. R. Kay, A. M. Brouwer, W. J. Buma, D. A. Leigh, and S. Woutersen, Science **328**, 1255 (2010).
[20]S. A. Vignon and J. F. Stoddart, Collect. Czech. Chem. Commun. **70**, 1493 (2005).
[21]P. Hamm and R. M. Hochstrasser, in *Ultrafast Infrared and Raman Spectroscopy*, edited by M. D. Fayer (Marcel Dekker, New York, 2001), pp. 273–347.
[22]A. Stolow and D. M. Jonas, Science **305**, 1575 (2004).
[23]A. Altieri, F. G. Gatti, E. R. Kay, D. A. Leigh, D. Martel, F. Paolucci, A. M. Z. Slawin, and J. K. Y. Wong, J. Am. Chem. Soc. **125**, 8644 (2003).
[24]K. Nakamoto, M. Margoshes, and R. E. Rundle, J. Am. Chem. Soc. **77**, 6480 (1955).
[25]G. C. Pimentel and A. L. McClellan, *The Hydrogen Bond* (Freeman, San Francisco, 1960).
[26]Y.-A. Yan, G. M. Krishnan, and O. Kühn, Chem. Phys. Lett. **464**, 230 (2008).
[27]S. Mukamel, *Principles of Nonlinear Optical Spectroscopy* (Oxford University Press, Oxford, 1995).
[28]G. Fleming and M. Cho, Annu. Rev. Phys. Chem. **47**, 109 (1996).
[29]P. Hamm, M. Lim, and R. M. Hochstrasser, Phys. Rev. Lett. **81**, 5326 (1998).
[30]M. Cho, J. Y. Yu, T. Joo, Y. Nagasawa, S. A. Passino, and G. R. Fleming, J. Phys. Chem. **100**, 11944 (1996).
[31]P. Bodis, R. Timmer, S. Yeremenko, W. J. Buma, J. S. Hannam, D. A. Leigh, and S. Woutersen, J. Phys. Chem. C **111**, 6798 (2007).
[32]T. Joo, Y. Jia, J.-Y. Yu, M. J. Lang, and G. R. Fleming, J. Chem. Phys. **104**, 6089 (1996).
[33]H. J. Eichler, P. Günter, and D. W. Pohl, *Laser-Induced Dynamic Gratings* (Springer, Berlin, 1986).
[34]See supplementary material at http://dx.doi.org/10.1063/1.3569761 for a description of the synthesis and characterization of the rotaxane.
[35]S. Yeremenko, M. S. Pshenichnikov, and D. A. Wiersma, Chem. Phys. Lett. **369**, 107 (2003).
[36]R. K. Pathria, *Statistical Mechanics* (Elsevier, Oxford, 1972).
[37]B. Henderson and G. F. Imbusch, *Optical Spectroscopy of Inorganic Solids* (Oxford University Press, New York, 1989).
[38]M. P. J. Brugmans, H. J. Bakker, and A. Lagendijk, J. Chem. Phys. **104**, 64 (1996).
[39]J. E. Sturm, J. Chem. Educ. **67**, 32 (1990).
[40]C. Fang, J. Wang, A. K. Charnley, W. Barber-Armstrong, A. B. Smith III, S. M. Decatur, and R. M. Hochstrasser, Chem. Phys. Lett. **382**, 586 (2003).
[41]D. Laage, H. Demirdjian, and J. T. Hynes, Chem. Phys. Lett. **405**, 453 (2005).
[42]A. Szabo, J. Chem. Phys. **81**, 150 (1984).
[43]J. T. Fourkas, R. Trebino, and M. D. Fayer, J. Chem. Phys. **97**, 78 (1992).
[44]For alternative models, see E. R. Smith, D. A. Farrow, and D. M. Jonas, J. Chem. Phys. **123**, 044102 (2005).
[45]J. Stenger, D. Madsen, P. Hamm, E. T. J. Nibbering, and T. Elsaesser, J. Phys. Chem. A **106**, 2341 (2002).
[46]S. Yeremenko, Ph.D. dissertation, University of Groningen, 2004.
[47]J. Park, J.-H. Ha, and R. M. Hochstrasser, J Chem. Phys. **121**, 7281 (2004).